

Predictability and Prediction of the North Atlantic Oscillation

Hai Lin

*Meteorological Research Division, Environment Canada
2121 Trans-Canada, Dorval, Quebec H9P 1J3, CANADA*

1. Introduction

The North Atlantic Oscillation (NAO) is one of the most important modes of variability in the Northern Hemisphere extratropical atmosphere. The NAO has a wide range of time scales from days to decades. It has larger amplitude in boreal winter than in summer. On interannual time scale, the NAO accounts for about 30% of the hemispheric surface air temperature variance over the past 60 winters (e.g., Hurrell 1996). The NAO has long been recognized as a major circulation pattern influencing the weather and climate from eastern North America to Europe.

It is generally accepted that the primary mechanism for the NAO is the internal dynamics of the extratropical circulation (Lau 1981; Limpasuvan and Hartmann 1999). This implies a lack of predictability for the NAO variability beyond the time scale of a baroclinic wave. Processes external to the extratropical atmosphere have also been found to contribute to the NAO variability on intraseasonal and seasonal scales. For example, tropical diabatic heating anomalies associated with the Madden-Julian Oscillation (MJO) can influence the extratropical circulation and the NAO (Cassou 2008; Lin et al. 2009). Sea surface temperature (SST) and snow cover anomalies may have an impact on the NAO on seasonal time scale (e.g., Rodwell et al. 1999; Cohen et al. 2001).

In this article, focus of discussion is made on the forecast skill of the NAO on intraseasonal and seasonal time scales.

2. Impact of the MJO

The Madden-Julian Oscillation (MJO) is the dominant mode of intraseasonal variability in the tropics, which is characterized by a large-scale zonal-vertical cell propagating eastward along the equator with a period of 30-60 days (e.g., Madden and Julian 1971). The maximum convective activity associated with the MJO occurs over the warm waters of the Indian Ocean and western Pacific where the signal moves eastward at a relatively slow speed (~5 m/s), whereas in the western hemisphere the MJO is less well coupled with convection and propagates faster (~15 m/s).

Through the variability of tropical diabatic heating, the MJO influences the extratropical circulations by driving teleconnection patterns. An important component in the coherent fluctuations between the tropical intraseasonal variability and the extratropical circulation is the possible link between the NAO and the MJO. To represent the MJO and its associated convection anomaly along the equator, eight phases were defined in Wheeler and Hendon (2004). Shown in Figure 1 is the composites of tropical precipitation rate anomaly for the eight phases of the MJO, calculated using the pentad CMAP data (Xie and Arkin 1997). Eastward propagation of the enhanced (red) and suppressed (blue)

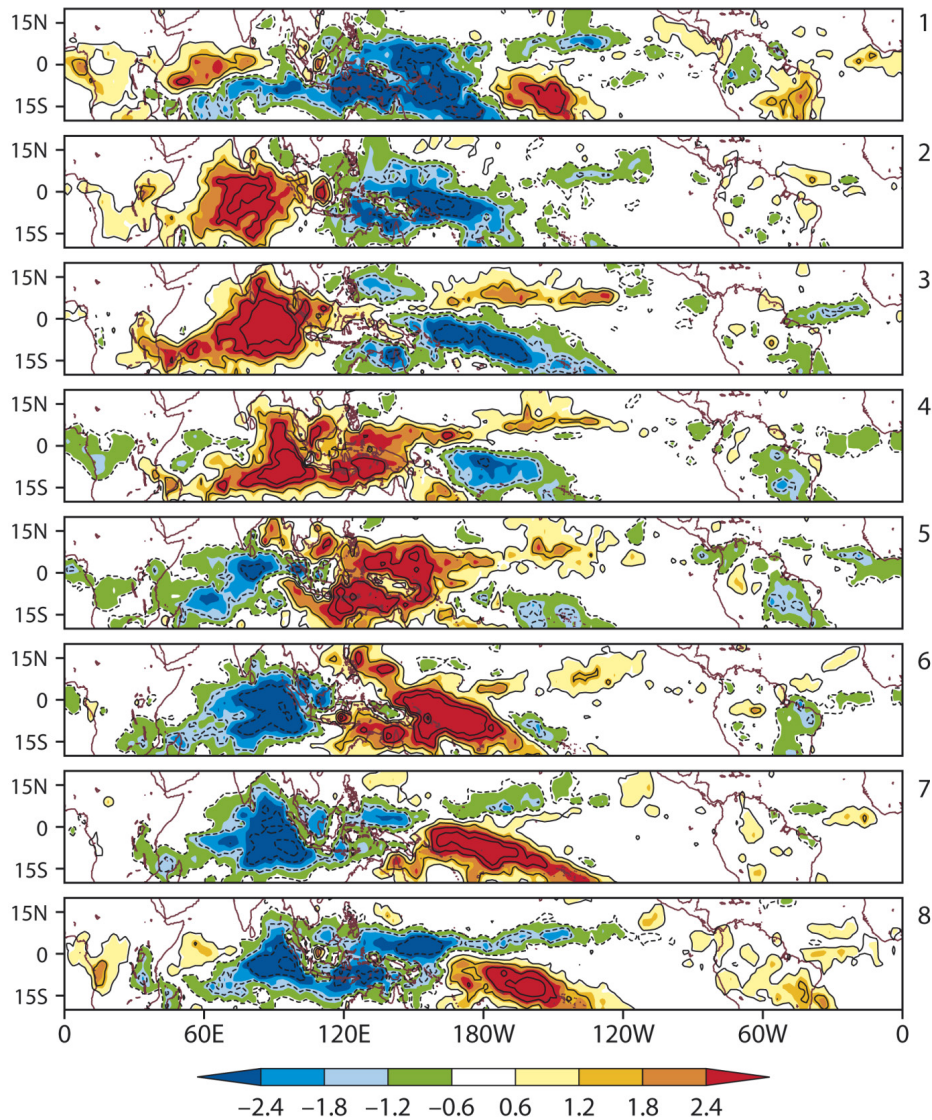


Figure 1: Simultaneous composites of the CMAP precipitation anomaly in the tropics for different MJO phases.

convections from the Indian Ocean to the central Pacific can be clearly seen for the MJO from Phases 1 to 8. Phases 2 and 3 (Phases 6 and 7) correspond to a dipole convection distribution with enhanced (suppressed) and suppressed (enhanced) precipitation centers over the eastern Indian Ocean and the western Pacific, respectively. As was discussed in detail in Lin et al. (2010a), the MJO phases of such a dipole equatorial convection distribution has a strong influence on the extratropical circulation and the NAO. Time-lagged composites and probability analysis of the NAO index for different phases of the MJO (Lin et al. 2009) reveal a statistically significant connection between the NAO and the tropical convection of the MJO. A significant increase of the NAO amplitude happens about 5 to 15 days after the MJO-related convection dipole anomaly develops in the tropical Indian Ocean and western Pacific region. Shown in Figure 2 are the lagged composite maps of 500-hPa geopotential height anomaly for MJO Phase 3 (upper panels) and Phase 7 (lower panels). Lag n indicates that the 500-hPa height anomaly lags the MJO of the specific phase by n pentads. About two pentads after MJO Phase 3 (Phase 7), a positive (negative) NAO is formed which can be traced back to the Rossby wave propagation originated from the North Pacific which is forced by the MJO diabatic heating anomaly.

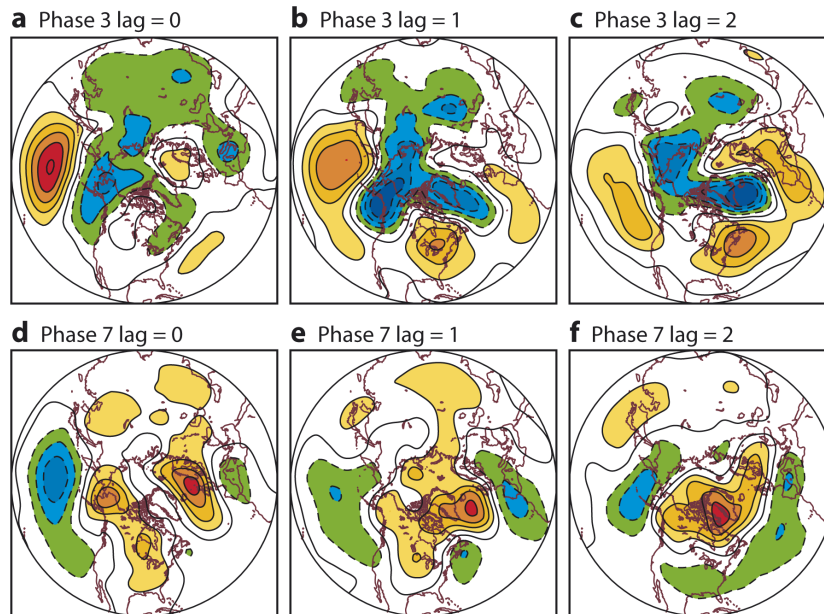


Figure 2: Lagged (in pentads) composites of 500-hPa geopotential height anomaly for MJO phase 3 (a-c) and phase 7 (d-f).

To study the association between the forecast skill of the NAO and the amplitude and phase of the MJO in the initial condition, the output of the intraseasonal hindcast experiment conducted with the Global Environmental Multiscale (GEM) model is analyzed. GEM is an operational atmospheric model at the Canadian Meteorological Centre (CMC) (Côté et al. 1998). An ensemble of 10 parallel integrations of 45 days is conducted for the 24 year period of 1985-2008 using GEM starting from the 1st, 11th and 21st of each month. As GEM is an atmospheric-only model, global sea surface temperatures (SST) are predicted using the persistence of the anomaly of the preceding 30 days. Forecasts that are initialized in the extended winter season (November to March) are analyzed. To measure the forecast skill of the NAO in the hindcast, correlation coefficient between the observed and forecast NAO indices is calculated. To see the dependence of NAO forecast skill on the MJO amplitude in the initial conditions, in Figure 3 the red and blue solid lines show the correlation skill of ensemble mean forecast of the NAO index for cases with strong and weak MJO signals at the initial state, respectively, where the strong and weak MJO are defined as those whose amplitude of the MJO index (RMM1 and RMM2) are greater and smaller than 1. Clearly, the NAO forecasts with a strong MJO in the initial condition perform better than those with a weak MJO. The biggest difference occurs at the third pentad of forecast. Shown in dashed red (blue) line is the average of skill calculated individually for each member for strong (weak) MJO initial conditions. The vertical bars represent the spread among the 10 members for each group, which is the standard deviation of the correlation skill for the members. For strong MJO cases, the spread of skill is smaller than that for the weak MJO cases at a given lead time. This indicates that the MJO signal also helps to reduce the uncertainty of the NAO forecast.

The forecasts can be grouped by the MJO phases corresponding to either a dipole or mostly a monopole tropical convection anomaly. The correlation skills of the NAO index for the forecasts with an MJO signal at the initial state that is in Phases 2, 3, 6 or 7 and in Phases 8, 1, 4, or 5 are compared. It is found that the NAO forecasts starting from a dipole tropical convection initial state have a better skill than those when the initial MJO has mostly a monopole convection structure. A detail discussion on the relationship between the MJO and the intraseasonal forecast of the NAO is given in Lin et al.

(2010b). These results indicate that it is possible to increase the skill of the NAO and the extratropical surface air temperature intraseasonal forecast with an improved tropical initialization, a better prediction of the tropical MJO and a better representation of the tropical-extratropical interaction in dynamical models.

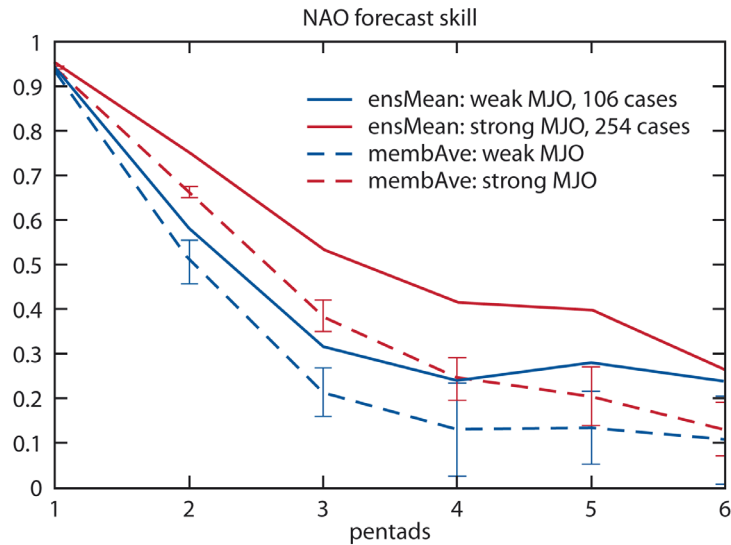


Figure 3: Correlation skill of the NAO index for strong MJOs (red line) and weak MJOs (blue line). Solid lines are for ensemble means, dashed lines are for the average value of correlation skill of the 10 individual members. Vertical bars represent standard deviation among 10 members.

3. Seasonal forecasts of the NAO

On seasonal time scale, possible signal sources for NAO variability are related to processes that are external to the atmosphere. Possible processes include the forcing from the underlying sea surface temperature (SST) anomaly in the extratropical North Atlantic (e.g., Palmer and Sun, 1985; Peng and Whitaker, 1999), coupling with the stratosphere (e.g., Baldwin et al. 2003), and interaction with the snow cover in Eurasia (e.g., Cohen et al. 2001). A link between the NAO and the diabatic heating in the tropics has been suggested by several studies (e.g., Lin et al. 2005; Li et al. 2006).

The output of the ensemble forecast experiments conducted under the second phase of the Historical Forecasting Project (HFP2) is analyzed to assess the seasonal forecast skill of the NAO. In HFP2, ensemble historical seasonal hindcast experiments were performed using four atmospheric GCMs, namely, the second and third generation atmospheric GCMs (GCM2 and GCM3) of the Canadian Centre for Climate Modelling and Analysis (CCCma; Boer et al. 1984), a reduced-resolution version of the global spectral model (SEF) of Recherche en prévision numérique (RPN; Ritchie 1991), and the GEM model of RPN/CMC. An ensemble of 10 parallel integrations of four-month duration was conducted for the 1969-2003 period using each model starting from the beginning of each month. The initial atmospheric conditions were at 12-hour intervals preceding the start of the forecasts, taken from the NCEP/NCAR reanalysis (Kalnay et al. 1996). Global sea surface temperatures (SST) were predicted using the persistence of the anomaly of the preceding month, i.e., the SST anomaly from the previous month was added to the climate of the forecast period. Sea ice extents were initialized with the analysis and relaxed to climatology over the first 15 days of integration.

Figure 4 depicts the correlation skill of the seasonal mean NAO index for each season (three-month average) with a 0-month lead time (months 1-3). The performances by different models are plotted in different colors. A score over about 0.3 can be treated as meaningful (0.05 significance level). For the NAO, there exists seasonal forecast skill in late winter to spring. The four models have a similar performance. Similar calculations for the forecasts at a 1-month lead time (months 2-4) do not show any skill for all the seasons (not shown).

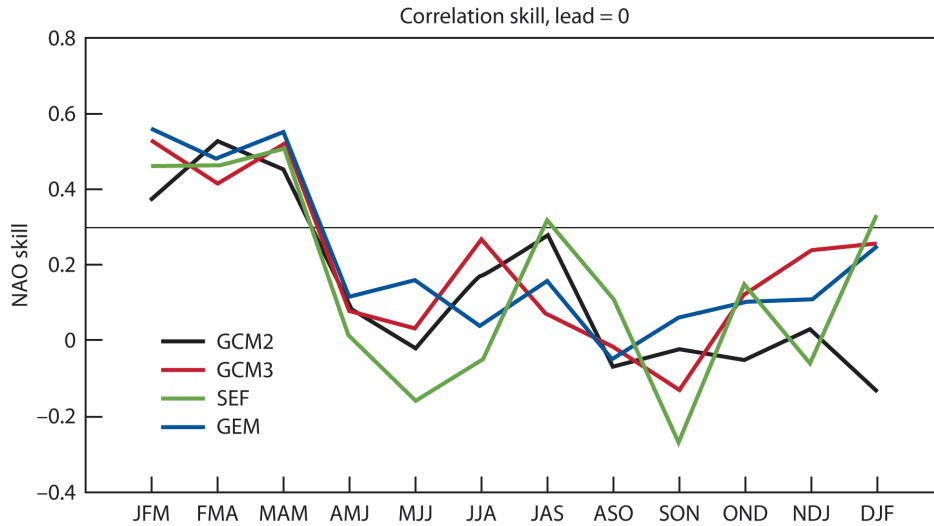


Figure 4: Correlation skill of the NAO for forecasts at a 0-month lead, as a function of forecast season.

It is possible that the NAO skill in the 0-month lead comes from the initial condition. Another explanation is that in the 1-month lead forecast the models do not produce a correct response pattern in the NAO. To explore this, the dominant forced patterns associated with tropical Pacific SST anomaly are identified using a singular value decomposition (SVD) analysis between November tropical Pacific SST and the ensemble mean Northern Hemispheric 500 hPa geopotential height averaged over two three-month segments (DJF which represents months 1-3 of the forecast, and JFM which is for months 2-4). To facilitate a comparison with the observations, a similar SVD calculation is performed on the observed 500 hPa geopotential height (Z500) and the same SST. This represents a lagged association between the observed height field and the tropical SST anomaly.

From the observed SVD patterns (Figure 5), SVD1 and SVD2 have similar Z500 distributions as the Pacific-North American (PNA) pattern and NAO, respectively. Thus, a positive PNA in JFM follows an above normal SST anomaly in the tropical eastern Pacific in November. Probably less familiar is the SST distribution for SVD2, which reveals a negative SST anomaly along the equatorial Pacific with a center in the middle and western tropical Pacific. The SVD analysis indicates that such an SST distribution in November leads to a positive NAO in JFM. Figure 6 shows the first and second pairs of SVD for the forecasts for GCM3. For SVD1 (Figure 6a), the forced PNA pattern is similar to the observations. The atmospheric component of SVD2, however, is far from the NAO pattern that is observed (Fig. 6b).

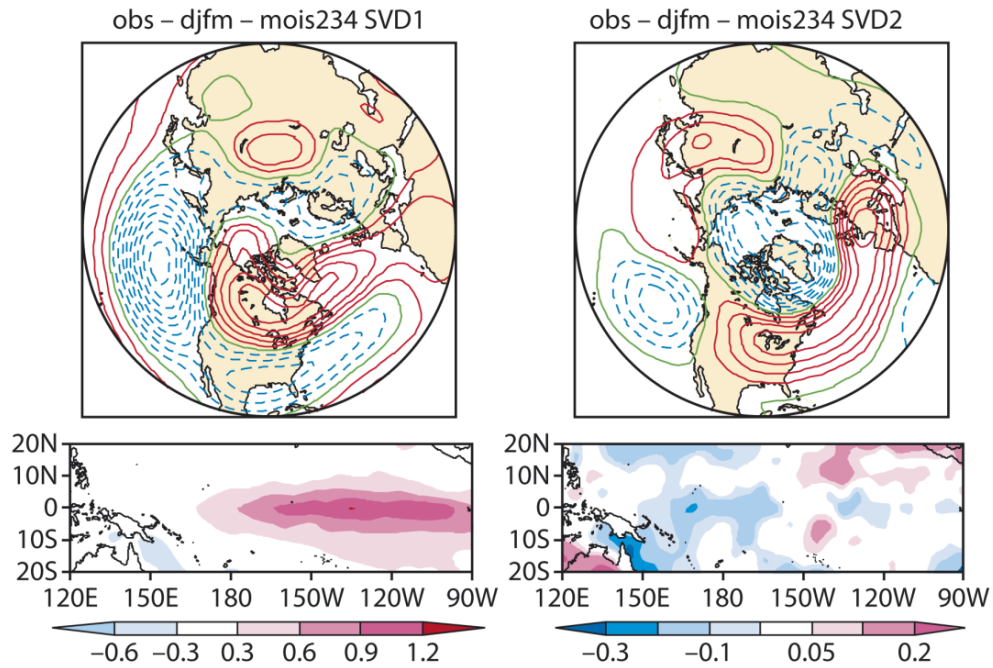


Figure 5: Observed JFM 500 hPa height (upper panels) and previous November SST (lower panels) distributions of SVD1 and SVD2.

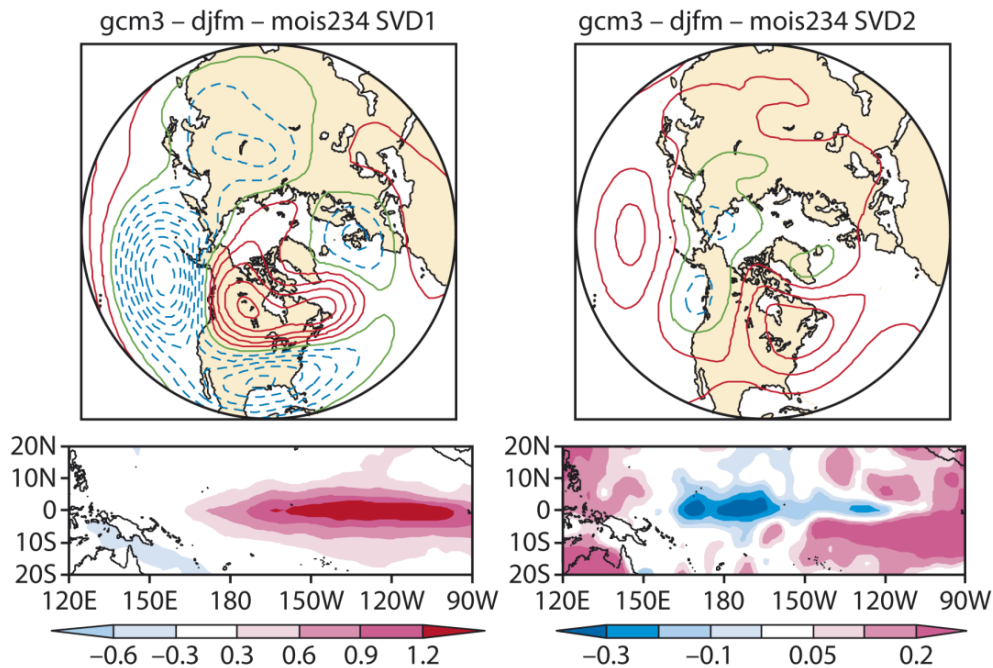


Figure 6: GCM3 ensemble forecast JFM 500 hPa height (upper panels) and previous November SST (lower panels) distributions of SVD1 and SVD2.

The SVD results for the other three models show similar features. The SST distributions of the first two modes have some similarities in the tropics among the four GCMs. The second SVD mode of atmospheric responses, however, is quite model dependent and biased. Interestingly, although the model spatial distribution of the SVD2 Z500 is very different from the NAO, its time variation (PC2) is significantly correlated with the NAO index. Table 1 lists temporal correlations for DJF (0-month

lead forecast) and JFM (1-month lead forecast). This result is striking, indicating that the NAO signal is embedded in the ensemble forecasts. Although the models cannot predict the NAO spatial pattern, the forced SVD2 has a time evolution that matched well the observed NAO index. Therefore, PC2 could be used as a skilful forecast of the NAO index. With this result, statistical postprocessing can be developed to improve seasonal forecasts (Lin et al. 2008, Jia et al. 2010).

Table 1: Columns 1 &2: correlations between the observed NAO index and the forecast NAO index (NAO skill). Columns 3 &4: correlations between the observed NAO index and the atmospheric expansion coefficients of SVD2. A correlation coefficient that is larger than 0.3 passes the 0.05 significance level which is shown in bold.

	Forecast NAO index		Forced SVD2	
	DFJ	JFM	DFJ	JFM
GCM2	-0.13	-0.30	0.30	0.35
GCM3	0.26	0.27	0.57	0.43
SEF	0.33	0.12	0.47	0.42
GEM	0.25	0.20	0.39	0.31

4. NAO hindcast with a simple GCM

In the above section, it was seen that GCMs usually have significant biases in producing the NAO spatial pattern that likely leads to a failure in NAO seasonal predictions. Two possible reasons are responsible for the error in the NAO forecast. Firstly, most GCMs have systematic biases in their simulated climatology. As is known, the generation and propagation of forced extratropical Rossby waves are sensitive to the basic flow. Secondly, seasonal forecasts in GCMs depend on anomalies of processes external to the atmosphere. Besides the SST anomaly, there are likely other processes that are important to force the NAO variability. These processes may not be well represented in the GCMs. Here we use a simple GCM (SGCM) to test if a numerical model with intermediate complexity can produce a skilful NAO seasonal forecast. This model, however, has a model climatology that closely matches that of the observations by construction, and has a forcing representation that includes a synthesis of all possible physical forcings: SST, sea-ice, land-surface conditions, etc.

Global forecasts were made for the 51 boreal winters [December–January–February (DJF)] from 1948/49 through 1998/99 with the SGCM. The latter uses a low-resolution spectral representation (T21) of the dry primitive equations, with five levels in the vertical. It is essentially the model first developed by Hoskins and Simmons (1975), to which Hall (2000) added time-independent forcing functions to the tendency equations and some linear damping of the momentum and thermo-dynamic equations. The forcing is obtained by computing the dynamical terms of the model, including the linear damping, with daily global analyses and setting the forcing equal to the residual term after averaging in time. The experimental protocol was designed to mimic that of an operational environment and HFP2, in that the forecast system used no information whatsoever from the DJF period to be forecast. Ensembles of 24 integrations were done for each of the 51 winters starting on 1 December. The forcing used for a given winter was the November-mean- forcing anomaly of that year added to the DJF-mean climatological forcing. The November forcing anomaly is assumed to persist through DJF.

As discussed in detail in Derome et al. (2005), the forecast skills of the SGCM and GCM2 (a more complex GCM used in HFP2) for the 500-hPa height for the same 26 DJF periods are comparable. The SGCM has skill generally in the same regions as the more complex model: the Tropics, the eastern North Pacific, western North America, the southeastern United States, part of the Arctic, and the eastern part of Asia.

We now look at the ensemble-mean forecast skill of the NAO index by SGCM during the 51 winters. The 0-month lead and 1-month lead forecasts both show significant skill (Table 2). A correlation skill of 0.44 was obtained for the NAO index, which is statistically significant at better than the 1% level. Interestingly, the correlation is higher than the value of 0.26 obtained for the PNA mode—a value that is significant only at the 7% level. This may seem surprising, as one might expect that the PNA, with its well known link to the tropical heating, would be the most predictable mode of variability. If we group the winters into strong and weak ENSO years, according to the amplitude of an ENSO index resulting in 16 winters of extreme phase of ENSO (EPSO) and 35 winters of non-extreme phase of ENSO (NEPSO), it is found that for EPSO winters, the PNA is much better forecast than the NAO, with a correlation of 0.68 between the SGCM predicted and observed PNA indices, while the NAO correlation does not pass the 10% significance level. During the NEPSO winters, the reverse holds. The NAO is skilfully predicted, but the PNA is not. The above correlations between observed and SGCM-predicted NAO and PNA time series were also calculated for January-February (JF; 1-month lead forecast). Table 2 shows that while the correlations are lower than for DJF, the main results are the same as for DJF.

Table 3 compares the SGCM’s skill in forecasting the NAO and PNA amplitudes with that of the GCM2 during the 26 winters that are common with the available GCM2 forecasts (1969–94). The results for the period 1969–94 are qualitatively similar to those for the longer period 1948–99, and SGCM and GCM2 agree with each other for the DJF forecast. For the forecast of JF, SGCM has a significant NAO forecast skill for all the winters and for the NEPSO winters. GCM2, however, has no

Table 2: Correlations between the observed and model ensemble mean the PNA and NAO indices. Numbers shown are those passing the 0.1 significance level, and those in bold passing the 0.05 significance level.

	DJF		JF	
	NAO	PNA	NAO	PNA
51 winters	0.44	0.26	0.34	
16 EPSO		0.68	0.39	0.59
35 NEPSO	0.46			

Table 3: Correlations between the observed and model ensemble mean the PNA and NAO indices. Numbers shown are those passing the 0.1 significance level, and those in bold passing the 0.05 significance level. Numbers outside (inside) of parentheses are for SGCM (GCM2).

	DJF		JF	
	NAO	PNA	NAO	PNA
26 winters	0.66 (0.47)	0.39 (0.34)	0.58 ()	0.43 (0.43)
9 EPSO		0.70 (0.67)		0.66 (0.84)
17 NEPSO	0.65 (0.58)		0.55 ()	

skill of NAO forecast with a 1-month lead time. A possible explanation is that the GCM2 response to external forcing has a biased NAO spatial pattern as discussed in last section, due to model's bias in climatology and an incomplete representation of forcing anomalies.

5. Summary

Predictions of the NAO on intraseasonal and seasonal time scales are discussed. On intraseasonal time scale, the NAO forecast skill is significantly influenced by the existence of the MJO signal in the initial condition. A strong MJO leads to a better NAO forecast skill than a weak MJO. An initial state with an MJO phase corresponding to a dipole tropical convection anomaly in the eastern Indian Ocean and western Pacific favours a more skilful NAO forecast than an MJO phase with a single tropical convection anomaly near the maritime continent. On seasonal time scale, some skilful NAO forecasts are possible in late winter and spring. In GCMs, the NAO as a response to boundary forcing has a biased spatial pattern, but the time evolution can be extracted with an SVD technique. This indicates that some statistical post-processing procedure can be used to improve the forecast skill. A simple GCM has a NAO seasonal forecast skill comparable to a more complex operational GEM forecast, which points to the importance of model climatology and representation of forcing.

Acknowledgements

I would also like to thank my colleagues, especially Drs. Gilbert Brunet and Jacques Derome, for their contribution in the related studies. I am grateful to members of the Canadian HFP project for making the seasonal hindcast available.

References

- Baldwin, M. P., D. B. Stephenson, D. W. J. Thompson, T. J. Dunkerton, A. J. Charlton, and A. O'Neill, 2003: Stratospheric memory and extended-range weather forecasts. *Science*, **301**, 636-640.
- Boer, G. J., N. A. McFarlane, R. Laprise, J. D. Henderson and J.-P. Blanchet, 1984: The Canadian Climate Centre spectral atmospheric general circulation model. *Atmosphere-Ocean*, **22**, 397-429.
- Cassou, C., 2008: Intraseasonal interaction between the Madden-Julian Oscillation and the North Atlantic Oscillation. *Nature*, **455**, 523-527.
- Cohen, J., K. Saito, and D. Entekhabi, 2001: The role of the Siberian high in Northern Hemisphere climate variability. *Geophys. Res. Lett.*, **28**, 299-302.
- Côté, J., S. Gravel, A. Méthot, A. Patoine, M. Roch, and A. Staniforth, 1998: The operational CMC-MRB Global Environmental Multiscale (GEM) model: Part I - Design considerations and formulation. *Mon. Wea. Rev.*, **126**, 1373-1395.
- Derome, J., H. Lin, G. Brunet, 2005: Seasonal forecasting with a simple General Circulation Model. *J. Climate*, **18**, 597-609.
- Jia, X., H. Lin, and J. Derome, 2010: Improving seasonal forecast skill of North American surface air temperature in fall using a post-processing method. *Mon. Wea. Rev.*, **138**, 1843-1857.
- Kalnay, E., M. Kanamitsu, R. Kistler, W. Collins, D. Deaven, L. Gandin, M. Iredell, S. Saha, G. White, J. Woolen, Y. Zhu, M. Chelliah, W. Ebisuzaki, W. Higgins, J. Janowiak, K. C. Mo, C. Ropelewski, J. Wang, A. Leetmaa, R. Reynolds, R. Jenne, D. Joseph, 1996: The NCEP/NCAR 40-year reanalysis project. *Bull. Amer. Meteor. Soc.*, **77**, 437-471.

- Hall, N. M. J., 2000: A simple GCM based on dry dynamics and constant forcing. *J. Atmos. Sci.*, **57**, 1557–1572.
- Hoskins, B. J., and A. J. Simmons, 1975: A multi-layer spectral model and the semi-implicit method. *Quart. J. Roy. Meteor. Soc.*, **101**, 637–655.
- Hurrell, J. W. , 1996: Influence of variations in extratropical wintertime teleconnections on Northern Hemisphere temperature. *Geophys. Res. Lett.*, **23**, 665-668.
- Lau, N.-C. , 1981: A diagnostic study of recurrent meteorological anomalies appearing in a 15-year simulation with a GFDL general circulation model. *Mon. Wea. Rev.*, **109**, 2287-2311.
- Limpasuvan, V., and D. L. Hartmann, 1999: Eddies and the annular modes of climate variability. *Geophys. Res. Lett.*, **26**, 3133-3136.
- Li, S., M. P. Hoerling, S. Peng, and K. M. Weickmann, 2006: The annular response to tropical Pacific SST forcing. *J. Climate*, **19**, 1802-1819.
- Lin, H., J. Derome, and G. Brunet, 2005: Tropical Pacific link to the two dominant patterns of atmospheric variability. *Geophys. Res. Lett.*, **32**, L03801, doi:10.1029/2004GL021495.
- Lin, H., G. Brunet, and J. Derome, 2008: Seasonal forecasts of Canadian winter precipitation by post-processing GCM integrations. *Mon. Wea. Rev.*, **136**, 769-783.
- Lin, H., G. Brunet, and J. Derome, 2009: An observed connection between the North Atlantic Oscillation and the Madden-Julian Oscillation. *J. Climate*, **22**, 364-380.
- Lin, H., G. Brunet, and R. Mo, 2010a: Impact of the Madden-Julian Oscillation on wintertime precipitation in Canada. *Mon. Wea. Rev.*, **138**, 3822-3839.
- Lin, H., G. Brunet, J. Fontecilla, 2010b: Impact of the Madden-Julian Oscillation on the intraseasonal forecast skill of the North Atlantic Oscillation. *Geophys. Res. Lett.*, **37**, L19803, doi:10.1029/2010GL044315.
- Madden, R. A., and P. R. Julian, 1971: Description of a 40-50 day oscillation in the zonal wind in the tropical Pacific. *J. Atmos. Sci.*, **28**, 702-708.
- Palmer, T. N., and Z. Sun, 1985: A modelling and observational study of the relationship between sea surface temperature in the northwest Atlantic and atmospheric general circulation. *Quart. J. Roy. Meteor. Soc.*, **111**, 947-975.
- Peng, S., and J. S. Whitaker, 1999: Mechanisms determining the atmospheric response to midlatitude SST anomalies. *J. Climate*, **12**, 1393-1408.
- Ritchie, H., 1991: Application of the semi-Lagrangian method to a multilevel spectral primitive-equation model. *Quart. J. Roy. Meteor. Soc.*, **117**, 91-106.
- Rodwell, M. J., D. P. Rowell, and C. K. Folland, 1999: Oceanic forcing of the wintertime North Atlantic Oscillation and European climate. *Nature*, **398**, 320-323.
- Wheeler, M., and H. H. Hendon, 2004: An all-season real-time multivariate MJO index: development of an index for monitoring and prediction. *Mon. Wea. Rev.*, **132**, 1917-1932.
- Xie, P., and P. A. Arkin. 1997: Global precipitation: A 17-year monthly analysis based on gauge observations, satellite estimates, and numerical model outputs. *Bull. Amer. Meteor. Soc.*, **78**, 2539-2558.